Supp. Figure Legends

Suppl. Figure 1. Chemical structure of LW106. Dashed area represents structural modification of lead compound 62.

Suppl. Figure 2. Tumor cell-derived *IDO1* expression level does not correlate with survival of two subtypes of lung cancer patients. Kaplan-Meier survival analysis of the relationship between survival rates and tumor cell-derived *IDO1* expression level in two subtypes of lung cancer patients. (**A, B**) Relationship between overall survival (OS) rate and *IDO1* expression level in lung adenocarcinoma (**A**) and squamous (**B**) patients. (**C, D**) Relationship between post-progression survival (PPS) rate and *IDO1* expression level in lung adenocarcinoma (**C**) and squamous (**D**) patients. Differences between two survival curves are measured by Log-Rank Test. *n* represents the number of patients.

Suppl. Figure 3. LW106 treatment inhibits IDO1 enzyme activity but does not affect tumor cell proliferation *in vitro*. (**A**) Inhibition rate of kynurenine (Kyn) for IFN-γ-stimulated HeLa cells that were treated with indicated concentrations of LW106 for 48 hrs (*n* = 3 independent experiments). (**B**) Western blot analysis of IDO1 protein levels for IFN-γ-stimulated HeLa cells that were treated with indicated compounds (results are representatives of three experiments). (**C**) Survival rate of indicated tumor cells that were treated with increasing doses of LW106. Cells were stained with trypan blue dye and the staining exclusive cells (*i.e.* live cells) were counted under light microscope. *n* = 3 independent experiments. (**D**) Representative images of cells as described in **C**. (**E**) Western blot analysis of IDO1 protein levels for B16F10 and Lewis cells (results are representatives of three experiments).

Suppl. Figure 4. LW106 treatment reverses $CD8^+$ T-cell suppression mediated by $IDO1^+$ mature DCs. $IDO1^-$ immature DCs were treated with 50 ng/ml hIFN-γ and 1 μg/ml LPS for 2 days, and the obtained $IDO1^+$ mature DCs or $IDO1^-$ immature DCs were co-cultured with purified lymphocytes in the presence of vehicle, LW106 or epacadostat for additional 2 days. Co-cultured cells were harvested, stained with anti-CD8 antibody and subjected to FACS analysis. (**A**) Representative plot of FACS analysis. (B) Percentage of $CD8^+$ T cells in the co-culture system as described in A. n = 3 independent experiments. Statistical significance was evaluated by two-way ANOVA test (* $P < 0.05$; ** $P < 0.01$).

Suppl. Figure 5. LW106 treatment does not induce histological change in tumor-bearing mice. (**A, B**) H.E. staining of vital organs from LW106-trated mice bearing with Lewis tumor cells (**A**) and B16F10 melanoma cells (**B**). Images are representative of images from six mice.

Suppl. Figure 6. LW106 treatment enhances infiltration and accumulation of T cells in B16F10 tumors. B16F10 xenografts from vehicle-, LW106- and epacadostat-treated mice were harvested 18 days after tumor challenge and subjected to FACS and

immunofluorescent analyses. (**A**) Representative dot plots and percentage of $CD8^+$ effector T cells of total $CD45^+$ cells for vehicle-, LW106- and epacadostat-treated mice (*n* = 5 mice, each). (**B**) Percentage of $CD4^+Foxp3^+$ regulatory T cells expressing Ki67 for indicated mice as shown in *A*. (**C**) Ratio of $CD4^+Foxp3^-$ effector T cells to $CD4^+Foxp3^+$ regulatory T cells in tumors of indicated mice as shown in *A*. (**D**) Representative immunofluorescent images (*left panels*; images are representative of images from five mice) and percentage of $CD8^+$ T cells expressing Ki67 for tumors of indicated mice (*right panel*; 1000 ~ 2000 cells were counted in 10 random fields of each slide). Arrow head denotes $Ki67^+CD8^+$ cells. Statistical significance was evaluated by two-way ANOVA test (* $P < 0.05$; ** $P < 0.01$; # $P < 0.05$; N.S., not significant).

Suppl. Figure 7. LW106 treatment results in impaired proliferation and survival of B16F10 melanoma cells in tandem with reduced recruitment of tumor-associated stromal cells and deposition of extracellular matrix. B16F10 xenografted tumors from vehicle-, LW106- and epacadostat-treated mice were harvested 18 days after tumor challenge and analyzed by immunohistochemistry. (**A**) Representative immunohistochemical images (*left panels*; images are representative of images from six mice) and percentages of Ki67-, phospho-histone H3- and cleaved caspase 3-positive cells for tumors of indicated mice (*right panels*; 1000 ~ 2000 cells were counted in 10 random fields of each slide). (**B**) Representative immunofluorescent images (*left panels*; images are representative of images from six mice) and relative fluorescent intensities of type I collagen, CD31 and α-SMA (*right panels*; relative fluorescent intensities were calculated in 10 random fields of each slide) for tumors of indicated mice (*n* = 6 mice, each). Statistical significance was evaluated by two-way ANOVA test (* $P < 0.05$; ** $P < 0.01$; *** $P < 0.001$; N.S., not significant).

Suppl. Fig. 1

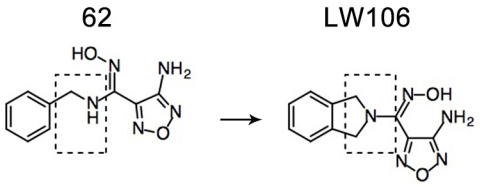

Suppl. Fig. 2

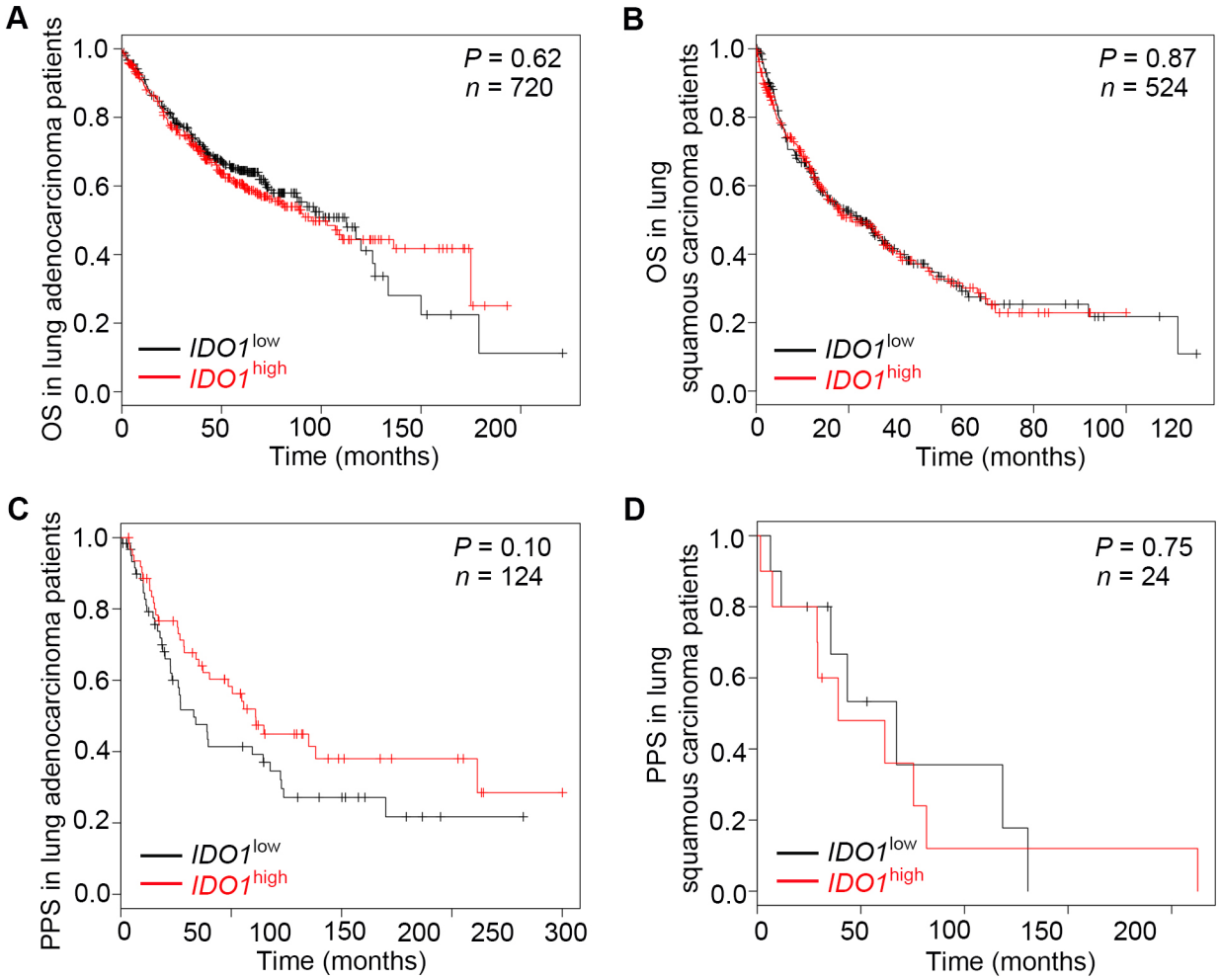
A
OS in lung adenocarcinoma patients
P = 0.62
n = 720
IDO1low
IDO1high
Time (months)
B
OS in lung squamous carcinoma patients
P = 0.87
n = 524
IDO1low
IDO1high
Time (months)
C
PPS in lung adenocarcinoma patients
P = 0.10
n = 124
IDO1low
IDO1high
Time (months)
D
PPS in lung squamous carcinoma patients
P = 0.75
n = 24
IDO1low
IDO1high
Time (months)

Suppl. Fig. 3

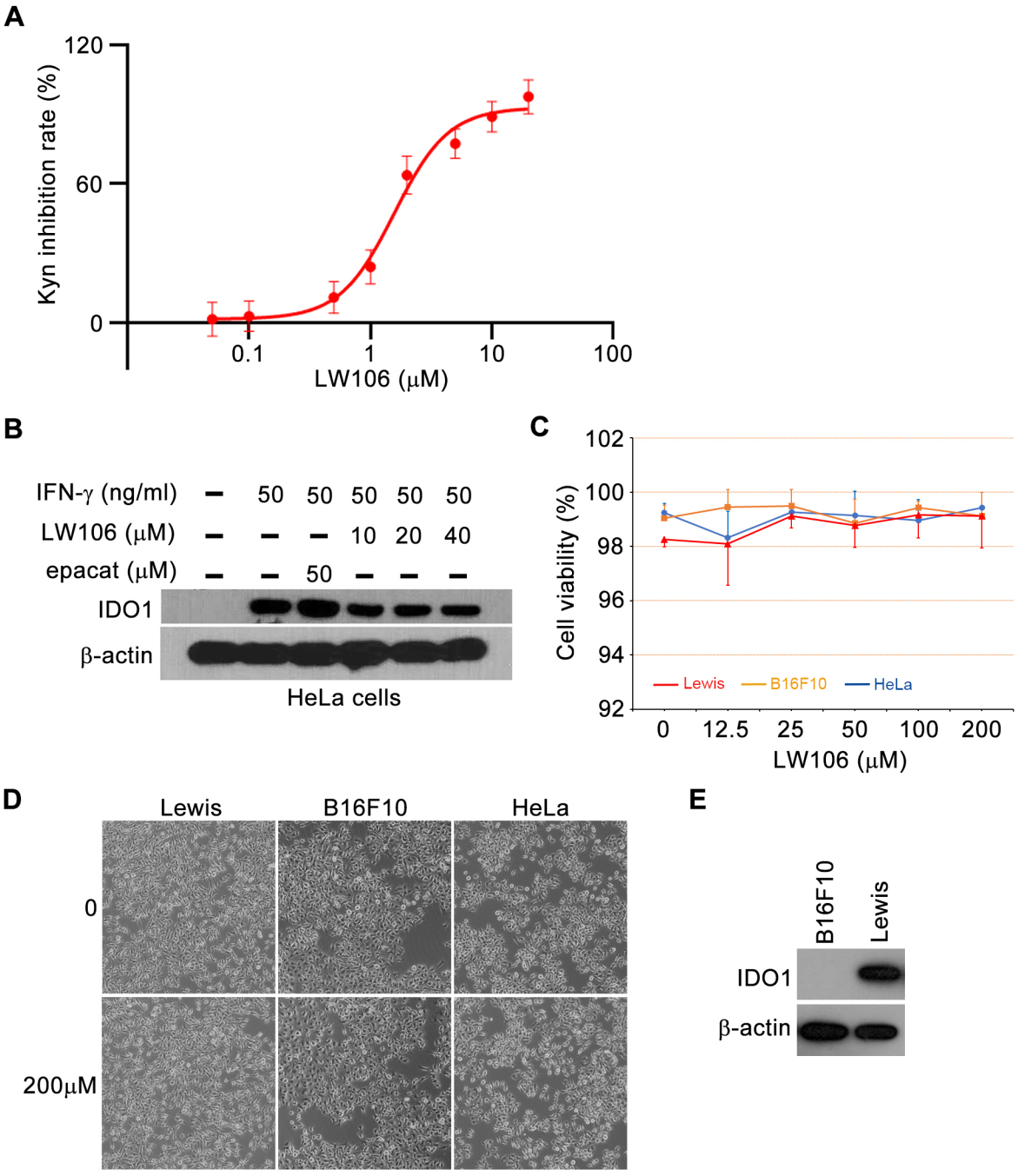
A
120
60
0
Kyn inhibition rate (%)
0.1
1
10
100
LW106 (μM)
B
IFN-γ (ng/ml) – 50 50 50 50 50
LW106 (μM) – – – 10 20 40
epacat (μM) – – 50 – – –
IDO1
β-actin
HeLa cells
C
102
100
98
96
94
92
Cell viability (%)
Lewis
B16F10
HeLa
0
12.5
25
50
100
200
LW106 (μM)
D
Lewis
B16F10
HeLa
0
200μM
E
B16F10
Lewis
IDO1
β-actin

Suppl. Fig. 4

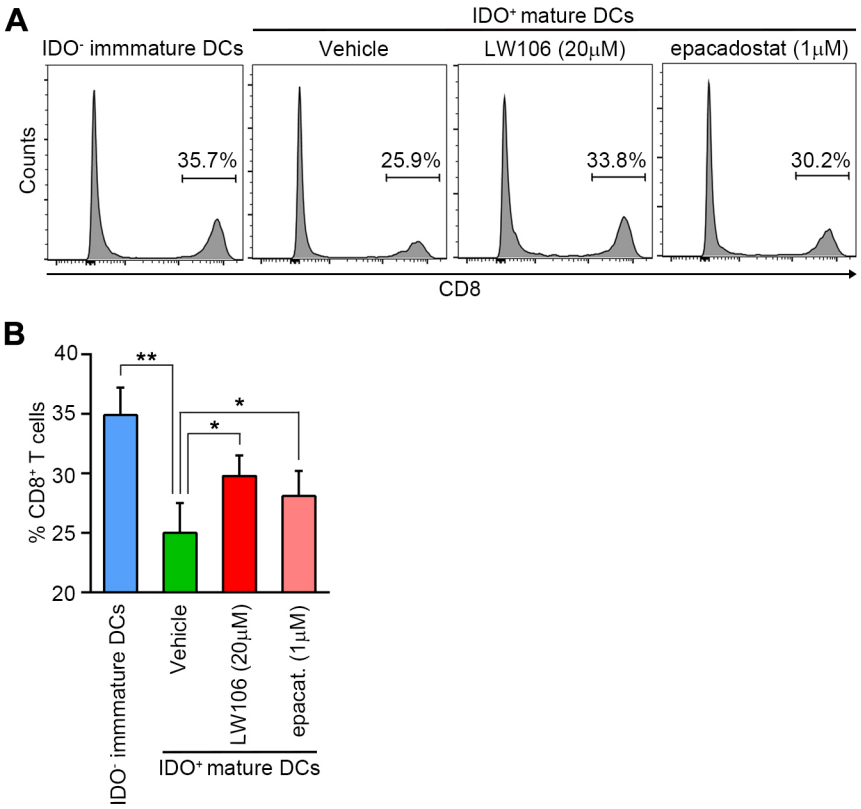
A
IDO+ mature DCs
IDO- immmature DCs
Vehicle
LW106 (20μM)
epacadostat (1μM)
Counts
35.7%
25.9%
33.8%
30.2%
CD8
B
% CD8+ T cells
40
35
30
25
20
**
*
*
IDO- immmature DCs
Vehicle
LW106 (20μM)
epacat. (1μM)
IDO+ mature DCs

Suppl. Fig. 5

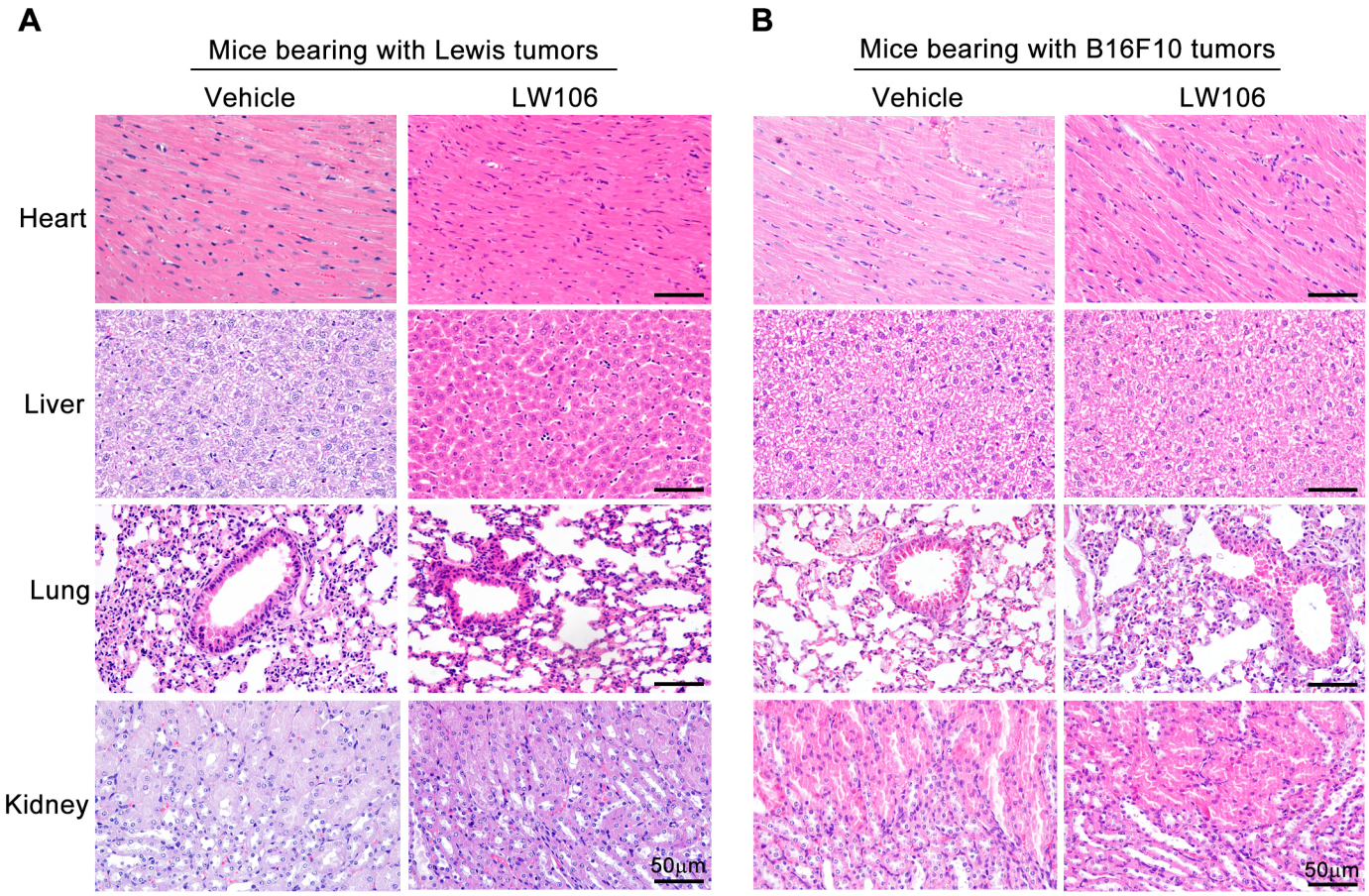
A
Mice bearing with Lewis tumors
Vehicle
LW106
Heart
Liver
Lung
Kidney
50μm
B
Mice bearing with B16F10 tumors
Vehicle
LW106
50μm

Suppl. Fig. 6

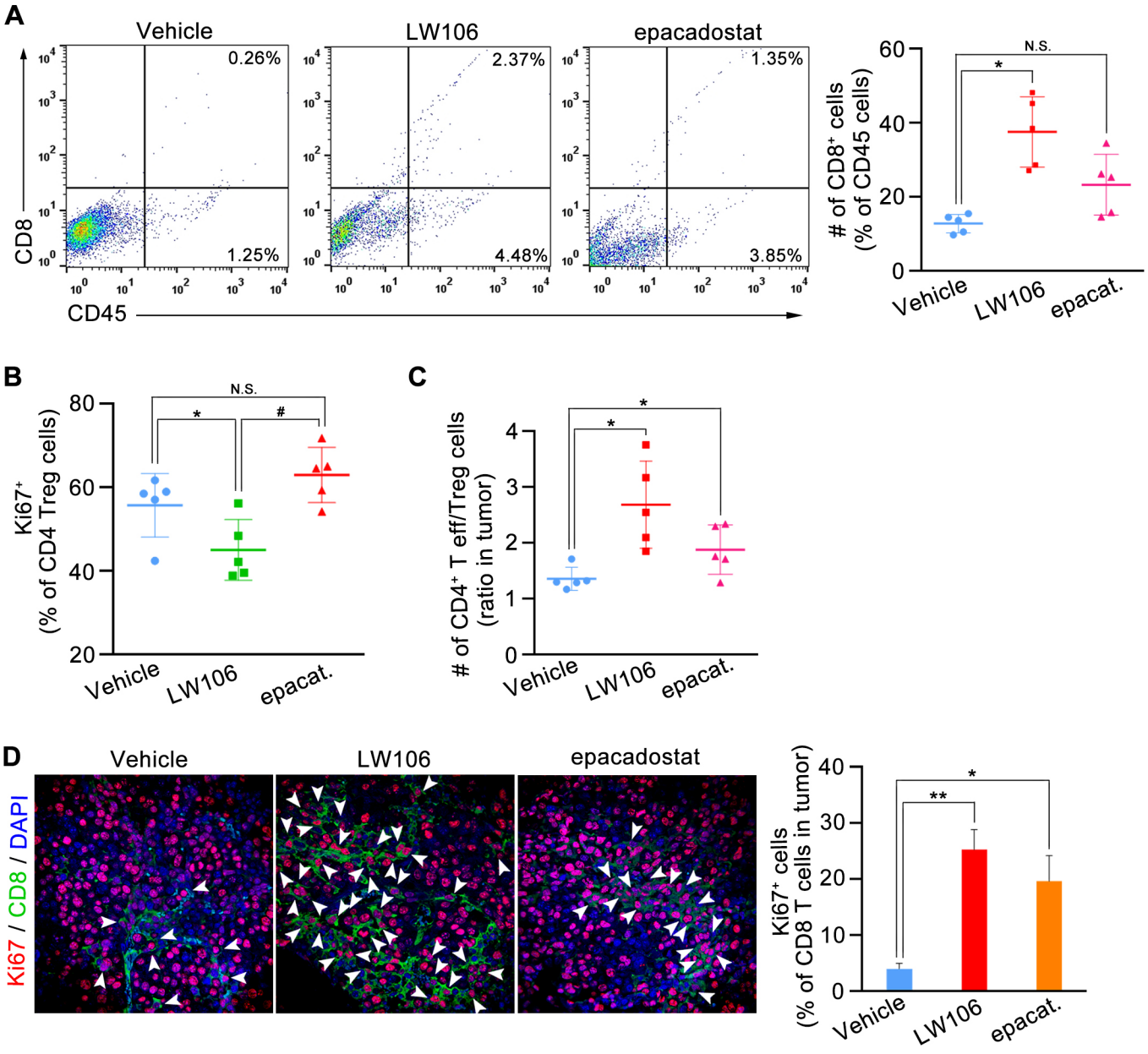
A
Vehicle
LW106
epacadostat
0.26%
1.25%
2.37%
4.48%
1.35%
3.85%
CD8
CD45
# of CD8⁺ cells (% of CD45 cells)
N.S.
*
Vehicle
LW106
epacat.
B
Ki67⁺ (% of CD4 Treg cells)
N.S.
*
#
C
# of CD4⁺ T eff/Treg cells (ratio in tumor)
D
Ki67 / CD8 / DAPI
Ki67⁺ cells (% of CD8 T cells in tumor)
**

Suppl. Fig. 7

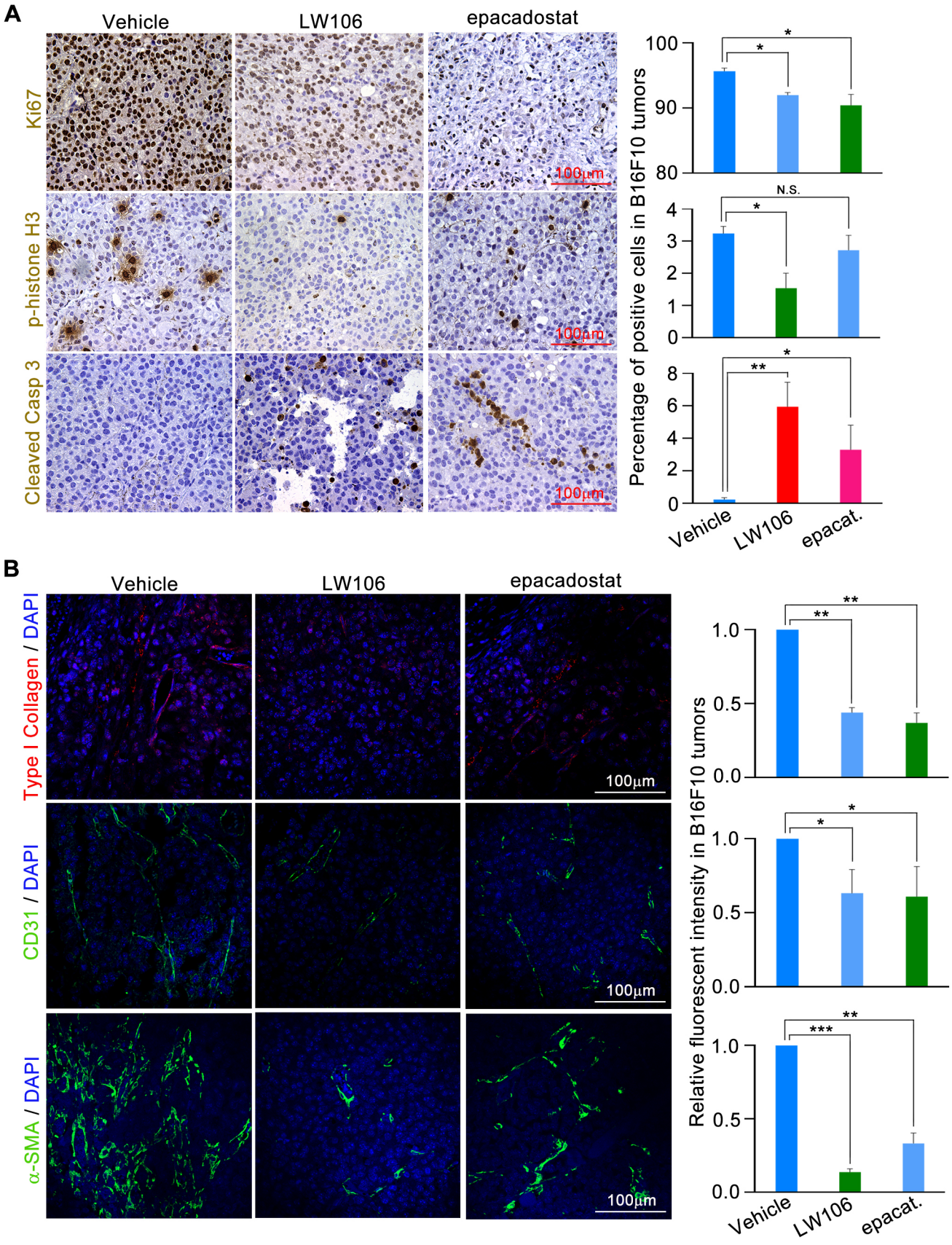
A
Vehicle
LW106
epacadostat
Ki67
p-histone H3
Cleaved Casp 3
100μm
Percentage of positive cells in B16F10 tumors
N.S.
Vehicle
LW106
epacat.
B
Vehicle
LW106
epacadostat
Type I Collagen / DAPI
CD31 / DAPI
α-SMA / DAPI
100μm
Relative fluorescent intensity in B16F10 tumors
Vehicle
LW106
epacat.